

GLOBAL DISTRIBUTION OF LUNAR IMPACT MELT FLOWS. C. D. Neish¹, J. Madden², L. M. Carter³, B. R. Hawke⁴, T. Giguere⁴, V. J. Bray⁵, G. R. Osinski⁶, and J.T.S. Cahill⁷, ¹The Florida Institute of Technology, Melbourne, FL, 32901 (cneish@fit.edu), ²Franklin and Marshall College, Lancaster, PA, 17603, ³NASA Goddard Spaceflight Center, Greenbelt, MD, 20770, ⁴The University of Hawai'i at Manoa, Honolulu, HI, 96822, ⁵The University of Arizona, Tucson, AZ, 85721, ⁶The University of Western Ontario, London, ON, N6A 3K7, ⁷The Johns Hopkins University Applied Physics Laboratory, Laurel, MD, 20723.

Introduction: Flow-like deposits of smooth, low albedo material interpreted to be impact melt rocks have been observed on the Moon, typically around young, fresh craters [1]. Melting is a fundamental part of the impact process, so the origin and emplacement of impact melt flows may provide important insights into the impact cratering process in general.

The launch of the Lunar Reconnaissance Orbiter (LRO) in June 2009 has afforded new views of lunar impact melt flows, allowing for a reassessment of their global distribution. Lunar impact melts have been primarily studied at optical wavelengths, but complementary information can be obtained by observing impact melts at radar wavelengths [2,3]. Since radar data is sensitive to surface and sub-surface roughness, it can be used to identify rough impact melt deposits, even when they are not easily seen in optical data.

In this work, we identified new impact melt flows using data from Mini-RF on LRO. This new survey provides a more complete global picture of lunar impact melt flows, allowing us to address fundamental questions about the emplacement of melt during the impact cratering process.

Observations: For each suspected impact melt deposit, we established the presence of melt at the crater in overlapping Lunar Reconnaissance Orbiter Camera (LROC) Narrow Angle Camera (NAC) images. We then determined the topography of the crater using Lunar Orbiter Laser Altimeter (LOLA) or LROC Wide Angle Camera (WAC) stereo data.

Distribution of melt-bearing craters. The data compiled in this work represents a total of 146 craters with exterior deposits of impact melt. This increases the known population of impact melt bearing craters by > 60% and allows us to reexamine the distribution and characteristics of impact melt deposits on the Moon. In general, the impact melt deposits identified in this work are more common in the highlands than the mare (Figure 1). Nelson et al. [4] mapped the mare regions on the Moon using a combination of LROC WAC and Clementine UVVIS mosaics, and found that mare regions constitute 18.7% of the area between 60°S and 60°N. Of the 146 impact melt bearing craters studied in this work, at most 10 of them lie in mare regions. If such craters were evenly spread about the Moon, we would expect ~24 of them to be in the mare. Thus, there is more than a factor of two discrepancy

between what we would expect to find in the mare and what is observed. One explanation is that the differing target properties of the highlands enhance the production of impact melt. The regolith dominated highlands are more porous than the more coherent mare surfaces [5]. Wünnemann et al. [6] predict a modest increase in melt production with increasing porosity, because of the lower critical shock pressures required for melting in porous materials.

In addition, the majority of craters in this study are smaller than 20 km in diameter. This is an unexpected result, since the limited amount of melt formed in small craters ($D < 10$ km) would likely be choked with cold clasts, increasing the melt's viscosity and chilling it rapidly [7]. Previous work suggested that small craters would have exterior melt deposits that do not extend far from the crater rim [1]. This new study shows the opposite – craters smaller than 10 km have the longest relative flow length of any size of crater on the Moon (Figure 2). A combination of pre-existing topography and oblique impact geometries may aid the melt emplacement in simple craters [1,8].

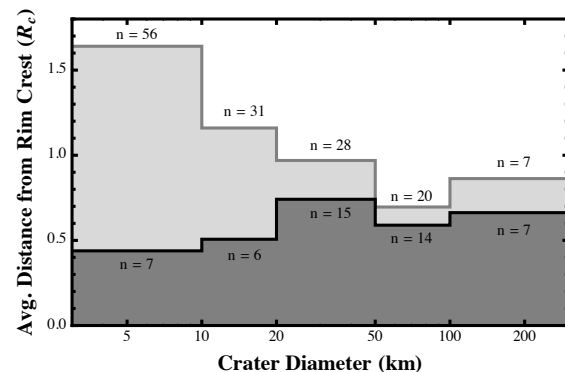


Figure 2: The average maximum distance that melt deposits occur from their parent crater rim, expressed in terms of crater radii, plotted for several diameter intervals. The dark gray histogram represents the original survey completed by [1]. The light gray histogram represents the present work.

Impact melt emplacement. This study also allows us to reexamine the relative role of pre-existing topography in melt emplacement. We separated the data set into simple craters (for this study, only those with $D \leq 10$ km) and complex craters (for this study, only those with $D > 20$ km), and determined the relative directions of the exterior impact melt deposits compared to the rim crest low.

For complex craters, we find a strong correlation between the direction of impact melt deposits and the rim crest low. Eighty percent of complex craters have melt flow directions that are within 45° of the rim crest low, and 53% coincide with the flow direction (Figure 3). One interpretation for this observation is that impact melt is emplaced during the modification stage of crater formation [1,8]. Uplift during cavity modification imparts an outward momentum to the melt-rich lining of the transient cavity, resulting in flow over the lowest point in the crater rim. After that point, the movement of melt – which is a fluid – will be largely controlled by the topography of the target region.

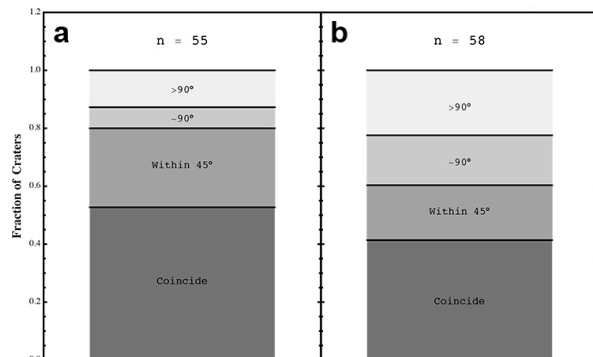


Figure 3: The correlation of the direction of the exterior impact melt deposits with the direction of the rim crest low for (a) complex and (b) simple craters.

For simple craters, there is no clear correlation with the rim crest low. Sixty percent of simple craters have melt directions that are within 45° of the rim crest low, and 41% coincide with the flow direction (Figure 3). Pre-existing topography and impact direction both

likely play a role in impact melt emplacement in simple craters, depending on the topography of the region (e.g., impact into crater rim or flat plain?) and the relative obliquity of the impact [8].

Conclusions: We analyzed the distribution and properties of 146 craters with impact melt deposits exterior to their rims. We find that most craters with exterior deposits of impact melt are small, ≤ 20 km, and that the smallest craters have the longest melt flows relative to their size. In addition, impact melt deposits are more common in the highlands than the mare, potentially suggesting that the porous highlands surface produces more melt than the more coherent mare surfaces. We find that 80% of complex craters and 60% of simple craters have melt directions that are coincident or nearly coincident with the lowest point in their rim, implying that pre-existing topography plays a dominant role in melt emplacement. This is likely due to movement during crater modification (complex craters) or breached crater rims (simple craters).

References: [1] Hawke B. R. and Head J. W. (1977) In: *Impact and explosion cratering*, Pergamon Press, New York, NY, pp. 815. [2] Campbell B. A. et al. (2010) *Icarus*, 208, 565. [3] Carter L.M. et al. (2012), *JGR*, 117, E00H09. [4] Nelson D.M. et al. (2013), *NLSI Forum*, 6. [5] Kiefer W.S. et al. (2012), *GRL*, 39, L07201. [6] Wünnemann K. et al. (2008), *EPSL*, 269, 530. [7] Cintala M.J. and Grieve R.A.F. (1998) *Meteoritics & Planet. Sci.*, 33, 889. [8] Osinski G.R. et al. (2011) *EPSC*, 310, 167.

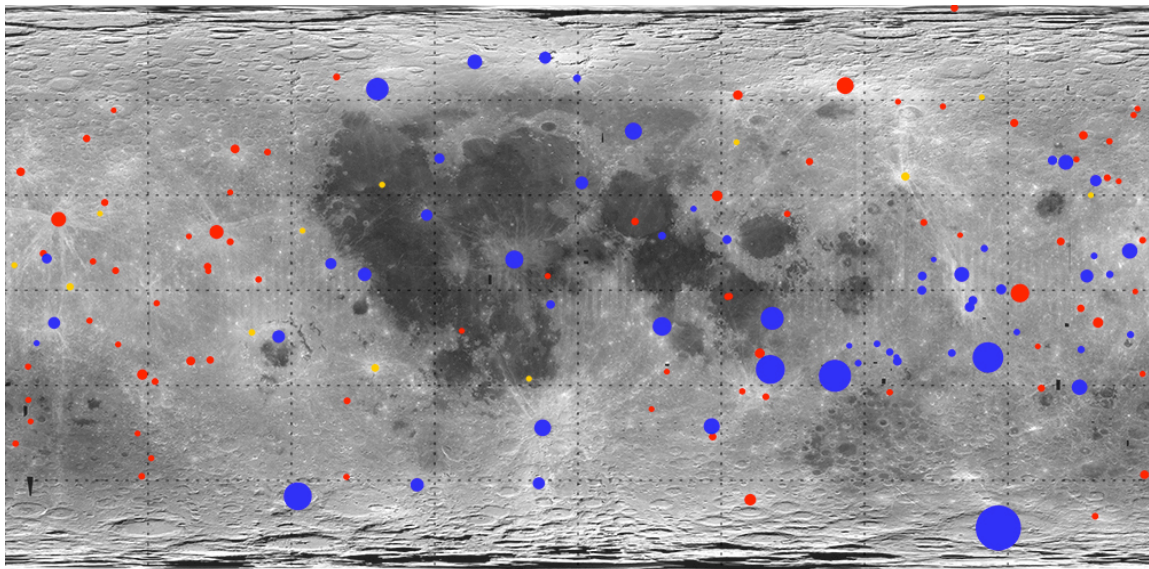


Figure 1: The position of lunar impact craters that possess exterior melt deposits, plotted over a Clementine UVVIS global mosaic. The size of the markers is scaled to crater diameter. Red markers are impact melts identified in Mini-RF data, yellow markers are impact melts identified in LROC publications, and blue markers are impact melts identified in pre-LRO publications.